Available online at www.sciencedirect.com
ScienceDirect
Ceramics International 36 (2010) 893–898
CERAMICS INTERNATIONAL
www.elsevier.com/locate/ceramint

Variation of discharge capacities with C-rate for $LiNi_{1-y}M_yO_2$ (M = Ni, Ga, Al and/or Ti) cathodes synthesized by the combustion method

SungNam Kwon [a], Soon-Do Yoon [b], HyeRyoung Park [b], MyoungYoup Song [c,*]

[a] Department of Hydrogen and Fuel Cells Engineering, Specialized Graduate School, Chonbuk National University, 664-14 Deogjindong 1-ga Deogjingu Jeonju, 561-756, Republic of Korea
[b] School of Applied Chemical Engineering, Chonnam National University, 300 Yongbongdong Bukgu Gwangju, 500-757, Republic of Korea
[c] Division of Advanced Materials Engineering, Research Center of Advanced Materials Development, Engineering Research Institute, Chonbuk National University, 664-14 Deogjindong 1-ga Deogjingu Jeonju, 561-756, Republic of Korea

Received 1 June 2009; received in revised form 15 September 2009; accepted 10 October 2009
Available online 13 November 2009

Abstract

$LiNiO_2$, $LiNi_{0.995}Al_{0.005}O_2$, $LiNi_{0.975}Ga_{0.025}O_2$, $LiNi_{0.990}Ti_{0.010}O_2$ and $LiNi_{0.990}Al_{0.005}Ti_{0.005}O_2$ specimens were synthesized by preheating at 400 °C for 30 min in air and calcination at 750 °C for 36 h in an O_2 stream. The variation of the discharge capacities with C-rate for the synthesized samples was investigated. $LiNi_{0.990}Al_{0.005}Ti_{0.005}O_2$ has the largest first discharge capacities at the 0.1 and 0.2 C rates. $LiNi_{0.990}Ti_{0.010}O_2$ has the largest first discharge capacity at the 0.5 C rate. In case of $LiNiO_2$ and $LiNi_{0.990}Ti_{0.010}O_2$, the first discharge capacity decreases slowly as the C-rate increases. $LiNiO_2$ has the largest discharge capacities at $n = 10$ (after stabilization of the cycling performance) at the 0.1, 0.2 and 0.5 C rates. This is considered to be related with the largest value of I_{003}/I_{104} and the smallest value of R-factor (the least degree of cation mixing) among all the samples. $LiNi_{0.975}Ga_{0.025}O_2$ exhibits the lowest discharge capacity degradation rates at 0.1, 0.2 and 0.5 C rates.

Keywords: $LiNi_{1-y}M_yO_2$ (M = Ni, Ga, Al and/or Ti); Combustion method; Discharge capacity; C-rate; Cycling performance

1. Introduction

Transition metal oxides such as $LiMn_2O_4$ [1–3], $LiCoO_2$ [4–6], and $LiNiO_2$ [7–10] have been intensively investigated in order to use them as the cathode materials of lithium secondary batteries. $LiMn_2O_4$ is comparatively inexpensive and does not bring about any environmental pollution, but its cycling performance is not adequate. $LiCoO_2$ has a large diffusivity and a high operating voltage, and it can be easily prepared. However, it has the disadvantage that it contains Co, an expensive element. $LiNiO_2$ is a very promising cathode material since it has a large discharge capacity [11] and it is excellent from the economic and environmental viewpoints. On the other hand, its preparation is very difficult compared with $LiCoO_2$ and $LiMn_2O_4$.

It is known that $Li_{1-x}Ni_{1+x}O_2$ forms rather than the stoichiometric $LiNiO_2$ during preparation [12] due to cation mixing. Excess nickel occupies the Li sites, destroying the ideally layered structure and preventing the lithium ions from undergoing the easy movement required for intercalation and deintercalation during cycling. This results in a small discharge capacity and poor cycling performance.

To improve the electrochemical properties of $LiNiO_2$, Co [13], Al [14,15], Ti [16], Ga [11], Mn [17] and Fe [18,19] were substituted for nickel by the synthesis in oxygen. Guilmard et al. [14] investigated the electrochemical performances of $LiNi_{1-y}Al_yO_2$ ($0.10 \leq y \leq 0.50$) specimens synthesized by a co-precipitation method. They showed that aluminum substitution suppressed all the phase transitions observed for the $LiNiO_2$ system. Chang et al. [16] detected partial disordering between the transition metal (Ni and Ti) layer and lithium by Rietveld refinement in $Li_xNi_{1-y}Ti_yO_2$ ($0.1 \leq y \leq 0.5$) prepared by solid-state reaction. By considering the ionic radius and the Ni–O bond length, they concluded that the Ni(II) ions are

* Corresponding author. Tel.: +82 63 270 2379; fax: +82 63 270 2386.
E-mail address: songmy@chonbuk.ac.kr (M. Song).

0272-8842/$36.00
doi:10.1016/j.ceramint.2009.11.009

partially stabilized in the lithium sites. Nishida et al. [11] reported that gallium-doping into $LiNiO_2$ stabilizes the crystal structure during the charging process and leads to better cycling performance than $LiNiO_2$.

$LiNiO_2$ synthesized by the solid-state reaction method does not have a high discharge capacity and has poor cycling performance, probably because it has poor crystallinity and non-uniform particle size. On the other hand, homogeneous mixing of the starting materials is possible in the combustion method because the starting materials are liquid. This may lead to good crystallinity and uniform particle size.

In this work, $LiNi_{1-y}M_yO_2$ (M = Ni, Ga, Al and/or Ti) specimens were synthesized by the combustion method, and the variation of the discharge capacities with C-rate for the synthesized samples was investigated.

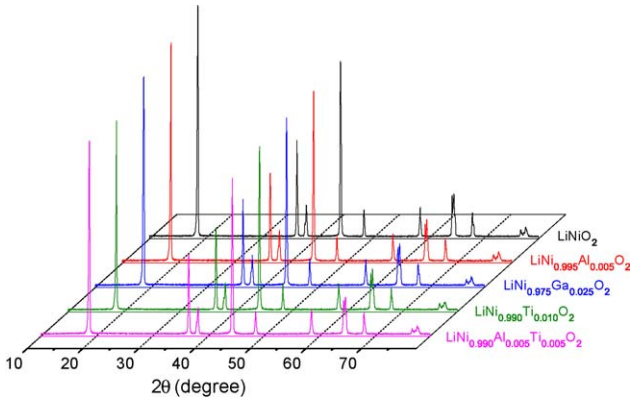

Fig. 1. XRD patterns of the synthesized materials $LiNiO_2$, $LiNi_{0.995}Al_{0.005}O_2$, $LiNi_{0.975}Ga_{0.025}O_2$, $LiNi_{0.990}Ti_{0.010}O_2$ and $LiNi_{0.990}Al_{0.005}Ti_{0.005}O_2$.

2. Materials and methods

Compositions $LiNiO_2$, $LiNi_{0.995}Al_{0.005}O_2$, $LiNi_{0.975}Ga_{0.025}O_2$, $LiNi_{0.990}Ti_{0.010}O_2$ and $LiNi_{0.990}Al_{0.005}Ti_{0.005}O_2$ were chosen because the specimens with these compositions showed relatively good electrochemical properties in our previous works [20,21]. Aldrich Chemical's $LiNO_3$, $Ni(NO_3)_2{\cdot}6H_2O$, $Al(NO_3)_2{\cdot}9H_2O$, $GaNO_3{\cdot}XH_2O$ and $Ti(NO_3)_4$ were used as starting materials. Excess lithium was added to compensate for the evaporated lithium during preparation. The excess lithium amount z in $Li_{1+z}Ni_{1-y}M_yO_2$ was 0.10. The starting materials, in the desired proportions, were dissolved in distilled water and mixed with urea by a magnetic stirrer. The mole ratio of urea to nitrate was 3.6. The mixture was heated to 400 °C in air and the temperature of 400 °C was maintained for 30 min. During that time the mixture formed ash by a combustion reaction. The ash was then pelletized and calcined at 750 °C for 36 h in an O_2 stream. The heating and cooling rates were about 100 °C h^{-1}. These synthesis conditions are the optimum ones to synthesize $LiNiO_2$ by the combustion method, studied in our previous work [22]. The phase identification of the synthesized samples was carried out by the X-ray powder diffraction analysis (Rigaku III/A diffractometer) using Cu Kα radiation, scanning rate of 6° min^{-1} and 2θ of $10° \leq 2\theta \leq 80°$. The electrochemical cells consisted of $LiNi_{1-y}M_yO_2$ as a positive electrode, Li foil as a negative electrode and an electrolyte [Purelyte (Samsung General Chemicals Co., Ltd.)] prepared by dissolving 1 M $LiPF_6$ in a 1:1 (volume ratio) mixture of ethylene carbonate (EC) and diethyl carbonate (DEC). The positive electrode consisted of synthesized materials, acetylene black and polyvinylidene fluoride (PVDF) binder dissolved in 1-methyl-2-pyrrolidinone (NMP) with a weight ratio of 85:10:5. A Whatman glass-filter was used as a separator. The coin-type (2016) cells were assembled in an argon-filled dry box. All of the electrochemical tests were performed at room temperature with a potentiostatic/galvanostatic system. The cells were cycled between 2.7 and 4.4 V at the rates of 0.1, 0.2 and 0.5 C.

3. Results and discussion

Fig. 1 shows the XRD patterns of the materials synthesized with excess lithium amount $z = 0.10$; $LiNiO_2$, $LiNi_{0.995}Al_{0.005}O_2$, $LiNi_{0.975}Ga_{0.025}O_2$, $LiNi_{0.990}Ti_{0.010}O_2$ and $LiNi_{0.990}Al_{0.005}Ti_{0.005}O_2$. All the samples possess the α-$NaFeO_2$ structure of the rhombohedral system (space group; $R\bar{3}m$) with no evidence of any impurities. The $R\bar{3}m$ structure is distorted in the c-axis direction of the hexagonal structure. This is reflected by the split of the 0 0 6 and 1 0 2 peaks and of the 1 0 8 and 1 1 0 peaks in the XRD patterns. The 0 0 6 and 1 0 2 peaks and the 1 0 8 and 1 1 0 peaks were split for all of the samples.

Ohzuku et al. [23] reported that electrochemically reactive $LiNiO_2$ showed a larger integrated intensity ratio of the 0 0 3 peak to the 1 0 4 peak ($I_{0\,0\,3}/I_{1\,0\,4}$) and a clear split of the 1 0 8 and 1 1 0 peaks in its XRD patterns. The degree of cation mixing (displacement of nickel and lithium ions) is low if the value of $I_{0\,0\,3}/I_{1\,0\,4}$ is large and the 1 0 8 and 1 1 0 peaks are split clearly. The value of $(I_{0\,0\,6} + I_{1\,0\,2})/I_{1\,0\,1}$, called the R-factor, is known to decrease as the unit cell volume of $Li_yNi_{2-y}O_2$ decreases. The R-factor increases as y in $Li_yNi_{2-y}O_2$ decreases for y near 1. This indicates that the R-factor increases as the degree of cation mixing becomes larger [7].

Table 1 shows the values of a, c, c/a, unit cell volume, $I_{0\,0\,3}/I_{1\,0\,4}$ and R-factor for the materials synthesized with excess

Table 1
Values of a, c, c/a, unit cell volume, $I_{0\,0\,3}/I_{1\,0\,4}$ and R-factor for the synthesized materials.

Samples	a (Å)	c (Å)	c/a	Unit cell volume (Å^3)	$I_{0\,0\,3}/I_{1\,0\,4}$	R-factor $[(I_{0\,0\,6} + I_{1\,0\,2})/I_{1\,0\,1}]$
$LiNiO_2$	2.881	14.209	4.932	102.146	1.319	0.459
$LiNi_{0.995}Al_{0.005}O_2$	2.880	14.205	4.931	102.067	1.287	0.505
$LiNi_{0.975}Ga_{0.025}O_2$	2.881	14.204	4.930	102.102	1.249	0.498
$LiNi_{0.990}Ti_{0.010}O_2$	2.881	14.209	4.932	102.146	1.160	0.470
$LiNi_{0.990}Al_{0.005}Ti_{0.005}O_2$	2.880	14.208	4.934	102.027	1.236	0.475

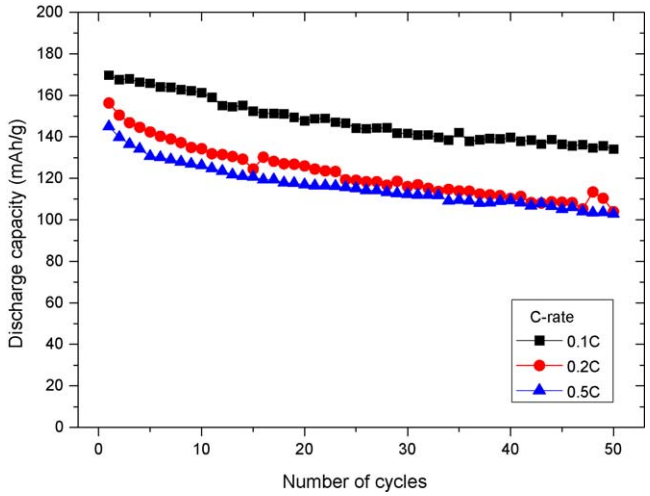

Fig. 2. Variation, with C-rate, of discharge capacity vs. number of cycles curve for the $LiNiO_2$ cathode.

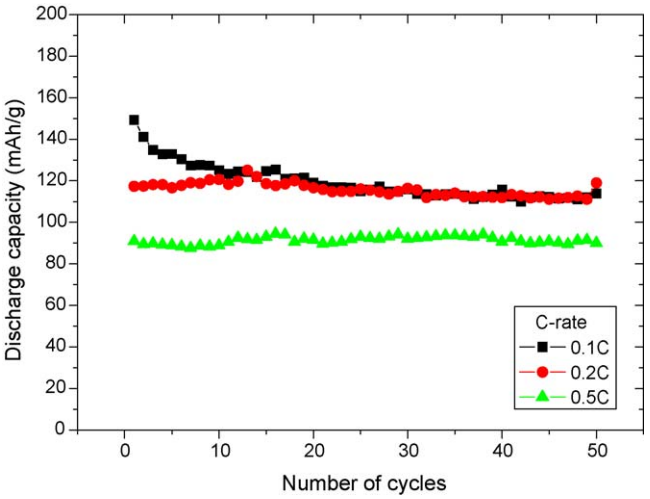

Fig. 4. Variation, with C-rate, of discharge capacity vs. number of cycles curve for the $LiNi_{0.975}Ga_{0.025}O_2$ cathode.

lithium amount $z = 0.10$. $LiNiO_2$ has the largest value of $I_{0\,0\,3}/I_{1\,0\,4}$ and its value decreases in the order of $LiNi_{0.995}Al_{0.005}O_2$, $LiNi_{0.975}Ga_{0.025}O_2$, $LiNi_{0.990}Al_{0.005}Ti_{0.005}O_2$ and $LiNi_{0.990}Ti_{0.010}O_2$. $LiNiO_2$ has the smallest value of R-factor and its value increases in the order of $LiNi_{0.990}Ti_{0.010}O_2$, $LiNi_{0.990}Al_{0.005}Ti_{0.005}O_2$, $LiNi_{0.975}Ga_{0.025}O_2$ and $LiNi_{0.995}Al_{0.005}O_2$. $LiNiO_2$ has the largest value of $I_{0\,0\,3}/I_{1\,0\,4}$ and the smallest value of R-factor.

Fig. 2 shows the variation, with C-rate, of discharge capacity vs. number of cycles curve for the $LiNiO_2$ cathode with the weight ratio of active material:acetylene black:binder = 85:10:5 (voltage range 2.7–4.4 V). The excess lithium amount z for the synthesis of $LiNiO_2$ was 0.10. The $LiNiO_2$ cathode has the largest first discharge capacity of 170 mAh/g at 0.1 C rate. The first discharge capacity decreases as the C-rate increases. The $LiNiO_2$ cathode exhibits the lowest discharge capacity degradation rate (0.66 mAh/g/cycle) and a discharge capacity at $n = 50$ of 103 mAh/g at 0.5 C rate. The $LiNiO_2$ cathode exhibits the discharge capacity degradation rate of 0.70 mAh/g/cycle and a discharge capacity at $n = 50$ of 134 mAh/g at 0.1 C rate.

Fig. 3 shows the variation, with C-rate, of discharge capacity vs. number of cycles curve for the $LiNi_{0.995}Al_{0.005}O_2$ cathode with the weight ratio of active material:acetylene black:binder = 85:10:5 (voltage range 2.7–4.4 V). The $LiNi_{0.995}Al_{0.005}O_2$ cathode has the largest first discharge capacity of 174 mAh/g at 0.1 C rate. The first discharge capacity decreases as the C-rate increases. At 0.2 C rate, the $LiNi_{0.995}Al_{0.005}O_2$ cathode exhibits the lowest discharge capacity degradation rate (0.37 mAh/g/cycle), the first discharge capacity of 135 mAh/g, and discharge capacity at $n = 50$ of 121 mAh/g. The $LiNi_{0.995}Al_{0.005}O_2$ cathode exhibits the discharge capacity degradation rate of 0.81 mAh/g/cycle and a discharge capacity at $n = 50$ of 123 mAh/g at 0.1 C rate.

Fig. 4 shows the variation, with C-rate, of discharge capacity vs. number of cycles curve for the $LiNi_{0.975}Ga_{0.025}O_2$ cathode. It has the largest first discharge capacity of 149 mAh/g at 0.1 C rate. The first discharge capacity decreases as the C-rate

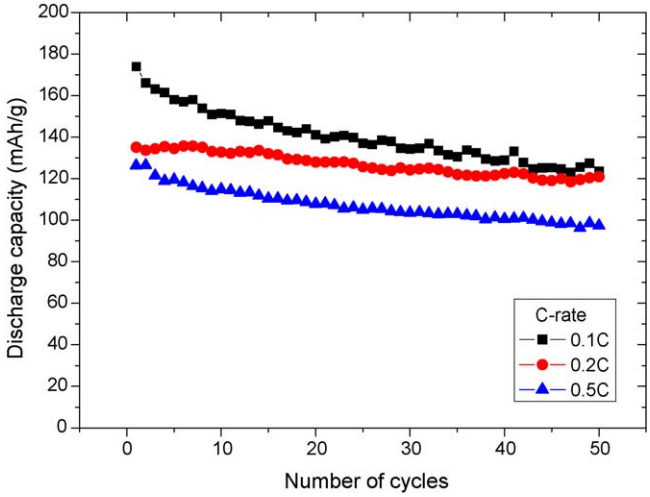

Fig. 3. Variation, with C-rate, of discharge capacity vs. number of cycles curve for the $LiNi_{0.995}Al_{0.005}O_2$ cathode.

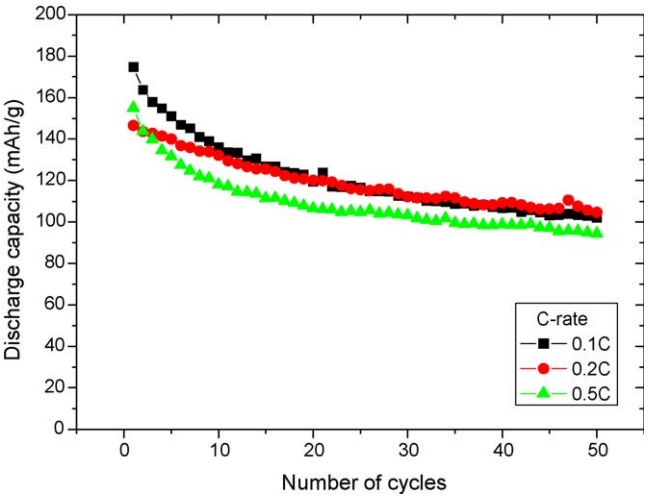

Fig. 5. Variation, with C-rate, of discharge capacity vs. number of cycles curve for the $LiNi_{0.990}Ti_{0.010}O_2$ cathode.

increases. The $LiNi_{0.975}Ga_{0.025}O_2$ cathode exhibits good cycling performances at 0.2 and 0.5 C rates from $n = 1$, and it has similar cycling performances at all the C-rates after $n = 10$. It shows very low discharge capacity degradation rates of 0.17 and 0.04 mAh/g/cycle, respectively, at 0.2 and 0.5 C rates. At 0.1 C rate, the $LiNi_{0.975}Ga_{0.025}O_2$ cathode exhibits the discharge capacity of 114 mAh/g at $n = 50$.

Fig. 5 shows the variation, with C-rate, of discharge capacity vs. number of cycles curve for the $LiNi_{0.990}Ti_{0.010}O_2$ cathode. The $LiNi_{0.990}Ti_{0.010}O_2$ cathode has the largest first discharge capacity of 175 mAh/g at 0.1 C rate. At 0.2 C rate, $LiNi_{0.990}Ti_{0.010}O_2$ exhibits the best cycling performance with the discharge capacity degradation rate of 0.77 mAh/g/cycle, and the discharge capacities at $n = 1$ and $n = 50$ are 147 and 105 mAh/g, respectively. It has similar cycling performances at all the C-rates after $n = 10$.

Fig. 6 shows the variation, with C-rate, of discharge capacity vs. number of cycles curve for the $LiNi_{0.990}Al_{0.005}Ti_{0.005}O_2$ cathode. It has the largest first discharge capacity of 185 mAh/g at 0.1 C rate. The first discharge capacity decreases as the C-rate increases. Its cycling performances are not good at all the C-rates with large discharge capacity degradation rates of 1.50, 1.45 and 0.90 mAh/g/cycle, respectively, at 0.1, 0.2 and 0.5 C rates. At 0.1 C rate, the $LiNi_{0.990}Al_{0.005}Ti_{0.005}O_2$ cathode exhibits the discharge capacity of 84 mAh/g at $n = 50$.

Fig. 7 shows the variation of the first discharge capacity with C-rate for the samples $LiNiO_2$, $LiNi_{0.995}Al_{0.005}O_2$, $LiNi_{0.975}Ga_{0.025}O_2$, $LiNi_{0.990}Ti_{0.010}O_2$ and $LiNi_{0.990}Al_{0.005}Ti_{0.005}O_2$. $LiNi_{0.990}Al_{0.005}Ti_{0.005}O_2$ has the largest first discharge capacities at the 0.1 and 0.2 C rates. $LiNi_{0.990}Ti_{0.010}O_2$ has the largest first discharge capacity at the 0.5 C rate. In case of $LiNiO_2$ and $LiNi_{0.990}Ti_{0.010}O_2$, the first discharge capacity decreases slowly as the C-rate increases. In case of $LiNi_{0.975}Ga_{0.025}O_2$ and $LiNi_{0.990}Al_{0.005}Ti_{0.005}O_2$, the first discharge capacity decreases relatively rapidly as the C-rate increases.

The curves of discharge capacity vs. number of cycles for all the samples show relatively rapid decrease from the first cycle

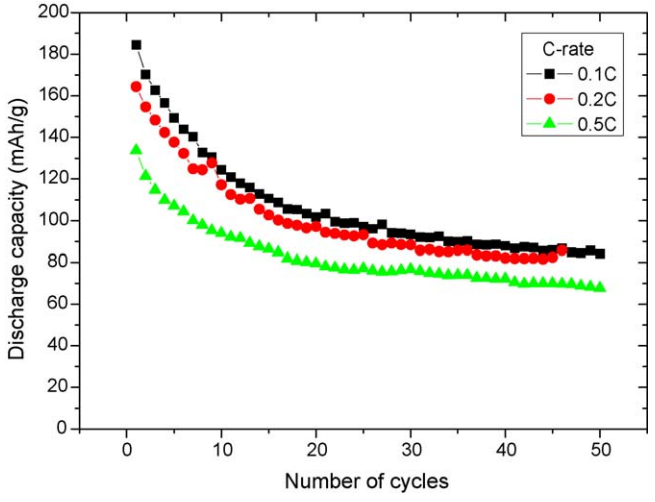

Fig. 6. Variation, with C-rate, of discharge capacity vs. number of cycles curve for the $LiNi_{0.990}Al_{0.005}Ti_{0.005}O_2$ cathode.

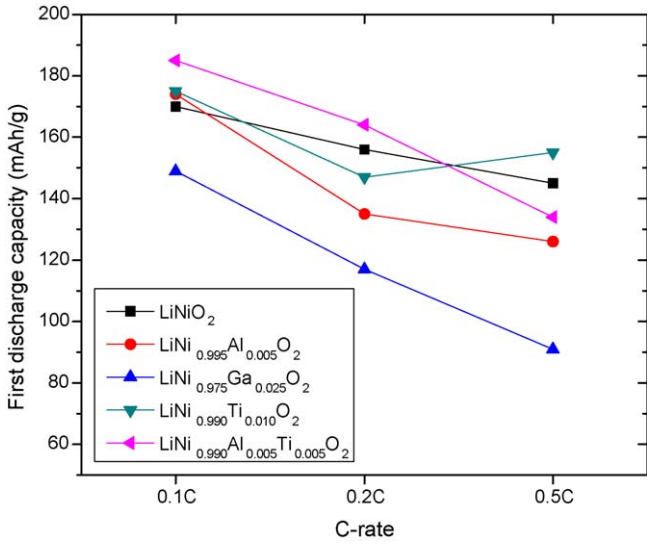

Fig. 7. Variation of the first discharge capacity with C-rate for the synthesized samples $LiNiO_2$, $LiNi_{0.995}Al_{0.005}O_2$, $LiNi_{0.975}Ga_{0.025}O_2$, $LiNi_{0.990}Ti_{0.010}O_2$ and $LiNi_{0.990}Al_{0.005}Ti_{0.005}O_2$.

up to $n = 10$, and thereafter slow decrease in the discharge capacity with the number of cycles, indicating that the cycling performance is stabilized after the 10th cycle. Fig. 8 shows the variation of the discharge capacity at $n = 10$ with C-rate for the samples $LiNiO_2$, $LiNi_{0.995}Al_{0.005}O_2$, $LiNi_{0.975}Ga_{0.025}O_2$, $LiNi_{0.990}Ti_{0.010}O_2$ and $LiNi_{0.990}Al_{0.005}Ti_{0.005}O_2$. $LiNiO_2$ has the largest discharge capacities at $n = 10$ at the 0.1, 0.2 and 0.5 C rates. This is considered to be related with the largest value of $I_{0\,0\,3}/I_{1\,0\,4}$ and the smallest value of R-factor (the least degree of cation mixing) among all the samples.

Fig. 9 shows the variation of the discharge capacity degradation rate from $n = 1$ to $n = 50$ with C-rate for the synthesized samples $LiNiO_2$, $LiNi_{0.995}Al_{0.005}O_2$, $LiNi_{0.975}Ga_{0.025}O_2$, $LiNi_{0.990}Ti_{0.010}O_2$ and $LiNi_{0.990}Al_{0.005}Ti_{0.005}O_2$. $LiNi_{0.975}Ga_{0.025}O_2$ exhibits the lowest discharge capacity

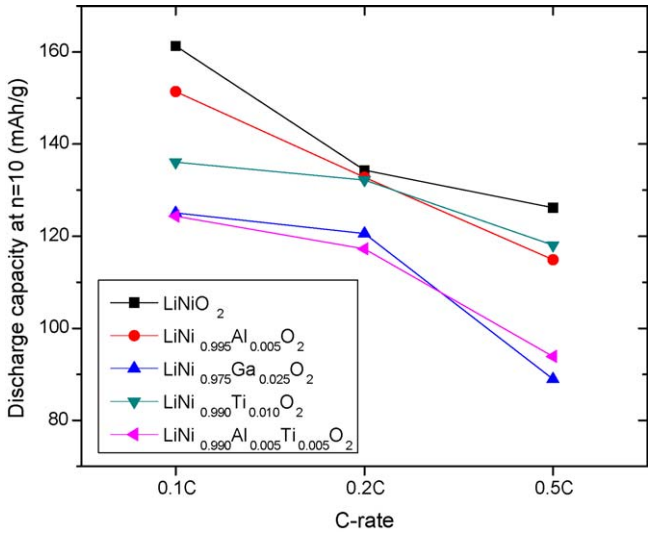

Fig. 8. Variation of the discharge capacity at $n = 10$ with C-rate for the synthesized samples $LiNiO_2$, $LiNi_{0.995}Al_{0.005}O_2$, $LiNi_{0.975}Ga_{0.025}O_2$, $LiNi_{0.990}Ti_{0.010}O_2$ and $LiNi_{0.990}Al_{0.005}Ti_{0.005}O_2$.

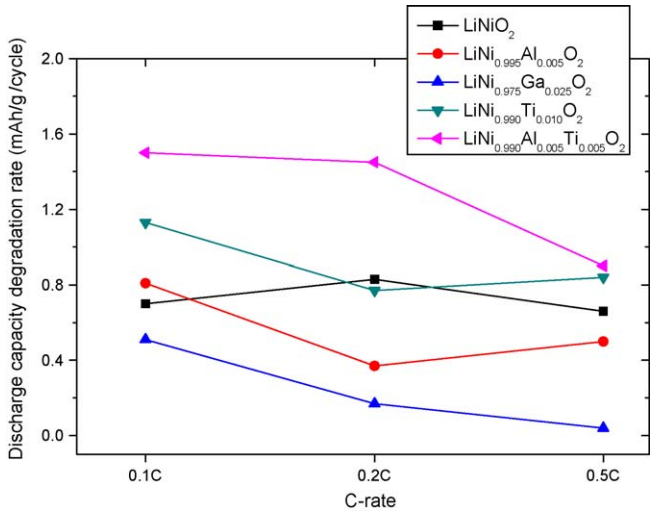

Fig. 9. Variation of the discharge capacity degradation rate from $n = 1$ to $n = 50$ with C-rate for the synthesized samples $LiNiO_2$, $LiNi_{0.995}Al_{0.005}O_2$, $LiNi_{0.975}Ga_{0.025}O_2$, $LiNi_{0.990}Ti_{0.010}O_2$ and $LiNi_{0.990}Al_{0.005}Ti_{0.005}O_2$.

degradation rates and $LiNi_{0.990}Al_{0.005}Ti_{0.005}O_2$ exhibits the highest discharge capacity degradation rates at 0.1, 0.2 and 0.5 C rates.

Fig. 10 shows the Coulombic efficiencies of the first cycle for the samples $LiNiO_2$, $LiNi_{0.995}Al_{0.005}O_2$, $LiNi_{0.975}Ga_{0.025}O_2$, $LiNi_{0.990}Ti_{0.010}O_2$ and $LiNi_{0.990}Al_{0.005}Ti_{0.005}O_2$ at 0.1, 0.2 and 0.5 C rates. $LiNi_{0.975}Ga_{0.025}O_2$ has relatively low Coulombic efficiencies (68.4, 71.6 and 62.5% at 0.1, 0.2 and 0.5 C rates, respectively). $LiNi_{0.990}Al_{0.005}Ti_{0.005}O_2$ has the highest Coulombic efficiencies (80.5, 80.8 and 72.7% at 0.1, 0.2 and 0.5 C rates, respectively).

All the synthesized samples $LiNiO_2$, $LiNi_{0.995}Al_{0.005}O_2$, $LiNi_{0.975}Ga_{0.025}O_2$, $LiNi_{0.990}Ti_{0.010}O_2$ and $LiNi_{0.990}Al_{0.005}Ti_{0.005}O_2$ possess the α-$NaFeO_2$ structure of the rhombohedral system (space group; $R\bar{3}m$) with no evidence of any impurities. In case of $LiNiO_2$ and $LiNi_{0.990}Ti_{0.010}O_2$, the first discharge capacity decreases slowly as the C-rate increases. In case of

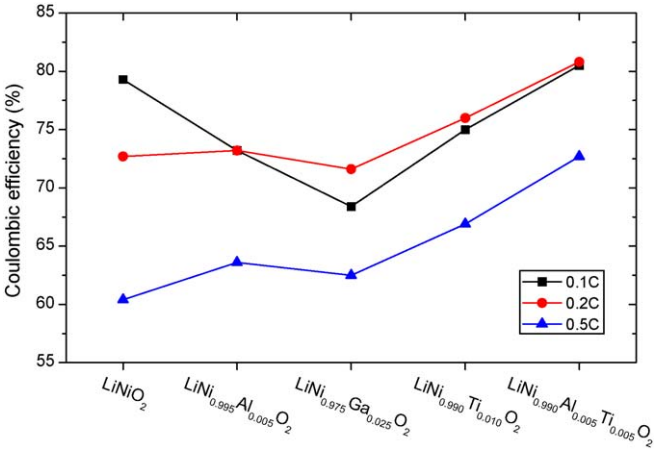

Fig. 10. Coulombic efficiencies of the first cycle for the samples $LiNiO_2$, $LiNi_{0.995}Al_{0.005}O_2$, $LiNi_{0.975}Ga_{0.025}O_2$, $LiNi_{0.990}Ti_{0.010}O_2$ and $LiNi_{0.990}Al_{0.005}Ti_{0.005}O_2$ at 0.1, 0.2 and 0.5 C rates.

$LiNi_{0.975}Ga_{0.025}O_2$ and $LiNi_{0.990}Al_{0.005}Ti_{0.005}O_2$, the first discharge capacity decreases relatively rapidly as the C-rate increases. $LiNiO_2$ has the largest discharge capacities at $n = 10$ (after stabilization of the cycling performance) at the 0.1, 0.2 and 0.5 C rates. This is considered to be related with the largest value of $I_{0\,0\,3}/I_{1\,0\,4}$ and the smallest value of R-factor (the least degree of cation mixing) among all the samples. $LiNi_{0.975}Ga_{0.025}O_2$ exhibits the lowest discharge capacity degradation rates at 0.1, 0.2 and 0.5 C rates.

4. Conclusions

$LiNiO_2$, $LiNi_{0.995}Al_{0.005}O_2$, $LiNi_{0.975}Ga_{0.025}O_2$, $LiNi_{0.990}Ti_{0.010}O_2$ and $LiNi_{0.990}Al_{0.005}Ti_{0.005}O_2$ specimens were synthesized by the combustion method, and the variation of the discharge capacities with C-rate for the synthesized samples was investigated. $LiNi_{0.990}Al_{0.005}Ti_{0.005}O_2$ has the largest first discharge capacities at the 0.1 and 0.2 C rates. $LiNi_{0.990}Ti_{0.010}O_2$ has the largest first discharge capacity at the 0.5 C rate. In case of $LiNiO_2$ and $LiNi_{0.990}Ti_{0.010}O_2$, the first discharge capacity decreases slowly as the C-rate increases. For $LiNi_{0.975}Ga_{0.025}O_2$ and $LiNi_{0.990}Al_{0.005}Ti_{0.005}O_2$, the first discharge capacity decreases relatively rapidly as the C-rate increases. $LiNiO_2$ has the largest discharge capacities at $n = 10$ (after stabilization of the cycling performance) at the 0.1, 0.2 and 0.5 C rates. This is considered to be related with the largest value of $I_{0\,0\,3}/I_{1\,0\,4}$ and the smallest value of R-factor (the least degree of cation mixing) among all the samples. $LiNi_{0.975}Ga_{0.025}O_2$ exhibits the lowest discharge capacity degradation rates at 0.1, 0.2 and 0.5 C rates.

Acknowledgements

This work was supported by grant No. R01-2003-000-10325-0 from the Basic Research Program of the Korea Science & Engineering Foundation. This paper was supported by the selection of research-oriented professor (M.Y. Song) of Chonbuk National University in 2009.

References

[1] J.M. Tarascon, E. Wang, F.K. Shokoohi, W.R. McKinnon, S. Colson, J. Electrochem. Soc. 138 (1991) 2859.
[2] A.R. Armstrong, P.G. Bruce, Lett. Nature 381 (1996) 499.
[3] M.Y. Song, D.S. Ahn, Solid State Ionics 112 (1998) 245.
[4] K. Ozawa, Solid State Ionics 69 (1994) 212.
[5] R. Alcántara, P. Lavela, J.L. Tirado, R. Stoyanova, E. Zhecheva, J. Solid State Chem. 134 (1997) 265.
[6] Z.S. Peng, C.R. Wan, C.Y. Jiang, J. Power Sources 72 (1998) 215.
[7] J.R. Dahn, U. von Sacken, C.A. Michal, Solid State Ionics 44 (1990) 87.
[8] J.R. Dahn, U. von Sacken, M.R. Jukow, H. Aljanaby, J. Electrochem. Soc. 138 (1991) 2207.
[9] A. Marini, V. Massarotti, V. Berbenni, D. Capsoni, R. Riccardi, E. Antolini, B. Passalacqua, Solid State Ionics 45 (1991) 143.
[10] W. Ebner, D. Fouchard, L. Xie, Solid State Ionics 69 (1994) 238.
[11] Y. Nishida, K. Nakane, T. Stoh, J. Power Sources 68 (1997) 561.
[12] J. Morales, C. Perez-Vicente, J.L. Tirado, Mater. Res. Bull. 25 (1990) 623.
[13] A. Rougier, I. Saadoune, P. Gravereau, P. Willmann, C. Delmas, Solid State Ionics 90 (1996) 83.

[14] M. Guilmard, A. Rougier, M. Grune, L. Croguennec, C. Delmas, J. Power Sources 115 (2003) 305.
[15] M.Y. Song, R. Lee, I.H. Kwon, Solid State Ionics 156 (2003) 319.
[16] S.H. Chang, S.G. Kang, S.W. Song, J.B. Yoon, J.H. Choy, Solid State Ionics 86–88 (1996) 171.
[17] M. Guilmard, L. Croguennec, C. Delmas, J. Electrochem. Soc. 150 (10) (2003) A1287.
[18] J.N. Reimers, E. Rossen, C.D. Jones, J.R. Dahn, Solid State Ionics 61 (1993) 335.
[19] R. Kanno, T. Shirane, Y. Inaba, Y. Kawamoto, J. Power Sources 68 (1997) 145.
[20] H.U. Kim, S.D. Youn, J.C. Lee, H.R. Park, C.G. Park, M.Y. Song, J. Korean Ceram. Soc. 42 (9) (2005) 631.
[21] H.U. Kim, S.D. Youn, J.C. Lee, H.R. Park, M.Y. Song, J. Korean Ceram. Soc. 42 (5) (2005) 352.
[22] M.Y. Song, I.H. Kwon, H.U. Kim, S. Shim, D.R. Mumm, J. Appl. Electrochem. 36 (2006) 801.
[23] T. Ohzuku, A. Ueda, M. Nagayana, J. Electrochem. Soc. 140 (1993) 1862.